Decay of ^{90}Kr

C. L. Duke
Physics Department, Grinnell College, Grinnell, Iowa 50112

W. L. Talbert, Jr.,* F. K. Wohn, and J. K. Halbig*
Ames Laboratory-DOE and Department of Physics, Iowa State University, Ames, Iowa 50011

K. Bonde Nielsen
Institute of Physics, University of Aarhus, Aarhus, Denmark
(Received 26 February 1979)

The β and subsequent γ decays of ^{90}Kr have been studied using an on-line isotope separator system. Ge(Li) γ-ray singles and γ-γ coincidence measurements were used to construct the level scheme for ^{90}Rb. This scheme has 31 excited states and includes 96 of the 103 observed γ-ray transitions. Spin and parity assignments have been deduced using β-decay log*ft* values from γ-ray intensity balances and internal conversion coefficients determined by on-line magnetic spectrometer measurements. Interpretation of some energy levels is made from a shell-model viewpoint.

[RADIOACTIVITY ^{90}Kr from ^{235}U(n,f); measured E and I for γ, *ce*; γ-γ coin. Ge(Li) detectors. Magnetic spectrometer. ^{90}Rb deduced ICC, multipolarities, levels, J, π, log*ft*. Mass-separated ^{90}Kr activity.]

I. INTRODUCTION

The study of the decay of ^{90}Kr has been in progress since 1969 at the TRISTAN on-line isotope separator. During this time, successive γ-ray measurements, each updating the previous results, were made using the best state-of-the-art detection systems. These γ-ray studies, coupled with magnetic spectrometer electron studies, have yielded a comprehensive decay scheme that includes 96 of the 103 observed transitions. These results are of interest due to the proximity of the daughter nucleus ^{90}Rb to the subshell and shell closures at $Z=38$ and $N=50$, respectively. A similar study of the decays of ^{90}Rb^{g,m} is nearing completion and will be reported in a later article.

The first comprehensive study of the ^{90}Kr decay using high-resolution detectors was published in 1970 by Mason and Johns.[1] In that report very preliminary results from this study were included; the final results reported here have resulted in a significantly modified decay scheme from that of Mason and Johns, particularly for the low-energy levels. Earlier work was adequately summarized by Mason and Johns.

Recently, Ekström *et al.*[2] measured the spins of the ^{90}Rb isomers. This information has been adopted in the discussion of the ^{90}Rb structure and departs from the spins previously adopted (the ground-state and isomer spins are reported in Ref. 2 to be 0 and 3, respectively, rather than 1 and 4, as previously assumed[3]).

The results reported here have already appeared in preliminary form in Nuclear Data Sheets.[3] The final results in this work are very similar but include changes in γ-ray intensities, minor changes in the decay scheme, and the inclusion of electron data (allowing model independent spin determinations). In addition, the ground-state β feeding from the ^{90}Kr decay has been recently determined to be $29\pm4\%$ ($27\pm5\%$ in the preliminary data reported in Nuclear Data Sheets[3]) by work at this laboratory.[4] The decay parameters adopted in Nuclear Data Sheets are $T_{1/2}=32.32\pm0.09$ s and $Q=4390\pm30$ keV. Direct measurements at this laboratory are 32.32 ± 0.09 s (Ref. 5) and 4390 ±40 keV.[6]

II. EXPERIMENTAL TECHNIQUES

A. Sample preparation

The $A=90$ activities were produced by thermal neutron fission of ^{235}U, followed by on-line mass separation with the TRISTAN facility at Ames Laboratory research reactor. At the time of these measurements, the ^{235}U target was connected to the oscillating electron ion source of the mass separator by a room-temperature transport line of length 1.6 m; thus, only gaseous fission products could reach the ion source. This configuration of the TRISTAN facility has been called TRISTAN I since the recent extension of the capabilities of TRISTAN to nongaseous activities.[7,8] TRISTAN I has been described in detail[9]; thus, only a few pertinent features need be mentioned here.

The $A = 90$ samples used in the present study had less than two parts in 10^5 of contaminating activities from neighboring masses. Some of the samples, however, had non-negligible amounts of ^{89}Kr arising from Kr hydride molecular ions present in the mass-separated ion beam.[9] The ^{89}Kr and ^{89}Rb decays were not serious contaminants since they have been well measured.[10] Furthermore, the ion source produced much less Kr hydride molecular ions than Kr ions and the $A = 89$ activities were only a small fraction of the total activity at $A = 90$.

B. γ-ray measurements

γ-ray singles and coincidence data were obtained from two Ge(Li) detectors having approximately 10% efficiency and 2.5-keV resolution (at 1332 keV). The two-parameter, buffer tape coincidence studies were performed using a 4096×4096 format, 180° detector orientation, and a 40-ns coincidence timing window. Approximately 10^7 coincidence events were recorded. Because of the importance of the low-energy part of the spectrum, a 1-cm^3 Ge(Li) low-energy photon spectrometer (LEPS) having 500-eV resolution (at 122 keV) was also used for singles and coincidence studies in conjunction with a 10% Ge(Li) detector. Spectra were taken with various enhancement factors determined by collection, delay, and count times at the moving tape collector in order to distinguish γ rays from ^{90}Kr from those of the ^{90}Rb^{g,m} daughter decays. This separation was not difficult since the ^{90}Rb decays have significantly longer half-lives and since the decays of ^{90}Rb were concurrently under study at this laboratory. All singles spectra were analyzed using standard computer-based methods. The gated spectra were analyzed both visually and by computer fitting techniques.

C. Electron measurements

High-resolution conversion electron measurements were made for the 106-keV doublet and the 121-keV doublet using the TRISTAN on-line magnenetic spectrometer.[11] The $A = 90$ conversion electron measurements have been described previously.[12] For these electron measurements the $\pi\sqrt{2}$ magnetic spectrometer was operated with a transmission of 0.3% and a momentum resolution full width at half maximum (FWHM) of 0.13%. This resolution corresponds to a FWHM of 370 eV for the K-conversion electrons of the 122-keV γ rays in the decay of ^{90}Kr. The electron sources were made on-line by depositing a narrow beam of $A = 90$ ions onto a thin (0.5 mg/cm^2) target of aluminized Mylar mounted at the source position of the spectrometer. Data were accumulated only with the deposited activity in equilibrium with the ion beam. This condition was critical since the two members of the 106-keV doublet have different half-lives. Equilibrium conditions were also maintained for the high-resolution γ-ray spectra which were used together with the electron spectra to obtain internal conversion coefficients.

III. EXPERIMENTAL RESULTS

A. γ-ray measurements

An $A = 90$ γ-ray spectrum with ^{90}Kr γ rays enhanced is shown in Fig. 1, in which the activity enhancement ratio of ^{90}Kr to ^{90}Rb is a factor of 40 larger than in an equilibrium $A = 90$ γ-ray spectrum. Table I lists the 103 γ rays that were assigned to the decay of ^{90}Kr. The coincidence relations established from the γ-γ coincidence measurements are given in Table II. In addition to the larger number of ^{90}Kr γ rays and corresponding γ-γ coincidence relations determined in the present study, the recognition of the doublet nature of the γ-ray peaks at 106 and 121 keV played a crucial role in departing from the level scheme of Mason and Johns.[1] The γ-ray and K-conversion electron peaks for the 122-keV doublet are shown in Fig. 2. Figure 3 shows the γ-ray and e^- peaks for the 106-keV doublet. In both figures the energy resolution (FWHM) is 570 eV for the γ rays and 370 eV for the conversion electrons.

B. Electron measurements

Internal conversion coefficients have been determined from the relative intensities of the peaks shown in Figs. 2 and 3, coupled with the combined intensities of the K-conversion electrons from the 121-keV doublet relative to the K-conversion intensity of the 106.9-keV isomeric transition for spectra taken with the ^{90}Kr and ^{90}Rb^{g,m} decays in equilibrium. This ratio, 14.6 ± 0.5, was previously reported in Ref. 12. The resulting internal conversion coefficients are given in Table III. The multipolarity of the 106.9-keV isomeric transition of ^{90}Rb^m was taken to be pure $M3$ since the recent results of Ekström *et al.*[2] yield a ground-state spin of 0 and a spin of 3 for the isomeric level. The choice of $M3$ rather than $E3$ for the isomeric transition is determined by the half-life and K/L intensity ratio. The K/L intensity ratio was found to be 6.2 ± 1.2 in the present work and 5.8 ± 1.1 from Ref. 13. The theoretical values[14] of 7.4 for $M3$ and 3.4 for $E3$ clearly dictate the choice of $M3$ on experimental grounds. Furthermore, the choice of $E3$ for the 106.9-keV tran-

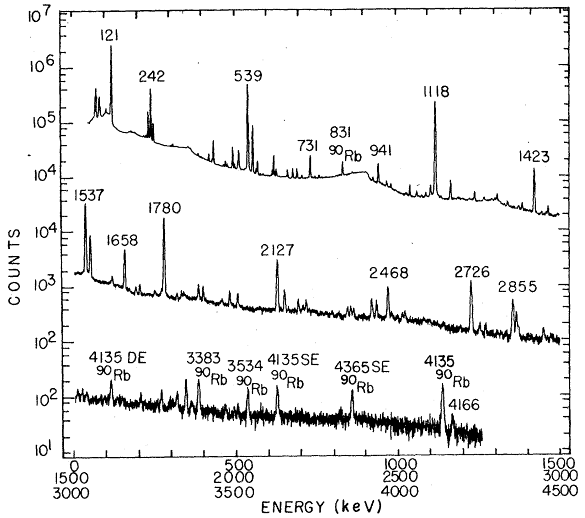

FIG. 1. ^{90}Kr-enhanced γ-ray spectrum.

sition would lead to inconsistencies in the multipolarities of the other three transitions in Table III, since these other transitions would still remain dominantly $M1$. Since the four transitions occur among the first four levels of ^{90}Rb (see the decay scheme of Fig. 4), there can be no self-consistent parity assignments if one of the transitions is $E3$ and the other three are $M1$. Thus the multipolarities listed in Table III are the only possibilities consistent with all experimental information. (It is worth pointing out that the large uncertainties for the internal conversion coefficients in Table III are due to the large uncertainty in the γ-ray intensity of the 106.9-keV transition relative to which all other internal conversion coefficients were calculated.)

C. Level scheme

The level scheme proposed for ^{90}Rb is shown in Fig. 4. The 31 levels were determined by comparing transition energy sums in agreement with the coincidence lists in Table II. A level was considered definite only if three or more transitions, or definite coincidence information, could be included with the level. The dashed levels were established on the basis of fewer than three associated transitions in the absence of definite coincidence information. Intensity balances to all excited states were used to calculate the absolute β branchings (based on a ground-state β feeding of $29 \pm 4\%$) and the $\log ft$ values shown in Table IV. The intensity balances were corrected for internal conversion using the experimental internal conversion coefficients listed in Table III or assumed theoretical $E1$ or $M1/E2$ values with equal mixture.

The major features of the scheme are the isomer at 106 keV and a strongly-fed (60%) level at 1780 keV depopulated by an intense triple cascade (1118-539-121 keV). The isomer, first discovered by Amarel *et al.*[15] in 1967, has an accepted half-life of 258 ± 5 s. The existence of this isomer is verified by the e^-, γ data shown in Fig. 3, which were used to establish the 106.9-keV transition as $M3$. The ordering of the 1118-539-121 triple cascade is uniquely determined by the coincidence information shown on the level scheme (Fig. 4) and in the coincidence list (Table II).

The major difference between the decay scheme presented here and that of Mason and Johns[1] is in the ordering of the 1118-539-121 cascade. Because Mason and Johns were unable to resolve the 121-keV doublet, they were forced by their coincidence data to assume the 1780-keV level was depopulated by two cascades of identical γ rays, 539-1118-121 and 1118-539-121, with the former carrying 69% of the total cascade intensity. In this work, LEPS-Ge(Li) coincidence gates on each member of the 121-keV doublet shown in Fig. 2 resolve the difficulties encountered by Mason and Johns. Thus, this study illustrates the importance of high-resolution singles and coincidence data for a unique determination of a complicated decay scheme.

Several other differences can be noted in the ^{90}Rb level scheme proposed by Mason and Johns[1] compared to this work. The 227-keV level in our level scheme is established on the basis of the coincidence observed between the 121.82- and 106.05-keV γ rays. The 676-keV level was not included in the scheme of Mason and Johns[1] because they did not interpret the 433-keV γ-ray peak as a doublet. It was apparent in this work that the intensity of the 433-keV peak in coincidence with the 242-keV transition was inconsistent with that expected from singles spectra. Furthermore, coincidences with both the 242- and 121-keV peaks demanded multiple placement for the 433-keV γ ray. Accordingly, this peak was reexamined in singles and the doublet nature indicated intensities consistent with the coincidence intensities for the placements suggested here.

There are many other levels presented in this work that are missing in the work of Mason and Johns, either because they failed to observe the γ-ray transitions involved or did not place them. Mason and Johns do report levels at 1240 and 1674 keV, but the 1118-539-121 cascade and 433-keV double placement in this work render these levels unnecessary.

TABLE I. Photopeaks observed in the decay of ^{90}Kr.

Energy (keV)	Relative intensity[a]	Placement (keV)	Energy (keV)	Relative intensity[a]	Placement (keV)
106.05 ± 0.03	11.5 ± 0.7	227 – 121	1118.69 ± 0.05	1000 ± 22	1780 – 661
106.92 ± 0.15	1.1 ± 0.3	106 – 0	1165.56 ± 0.06	21.2 ± 0.8	1780 – 614
120.92 ± 0.03	90 ± 6.0	227 – 106	1240.34 ± 0.11	9.0 ± 0.6	1901 – 661
121.82 ± 0.03	910 ± 30.0	121 – 0	1293.7 ± 0.4	1.5 ± 0.4	1400 – 106
180.66 ± 0.15	1.0 ± 0.5	536 – 356	1303.36 ± 0.24	2.4 ± 0.4	3083 – 1780
220.82 ± 0.14	1.0 ± 0.5	933 – 712	1309.68 ± 0.10	7.1 ± 0.4	
227.76 ± 0.08	3.2 ± 0.3	227 – 0	1341.31 ± 0.22	4.0 ± 0.5	1463 – 121
234.44 ± 0.03	68 ± 3.0	356 – 121	1386.62 ± 0.15	5.0 ± 0.5	2127 – 740
242.19 ± 0.03	255 ± 8.0	242 – 0	1423.77 ± 0.06	75.3 ± 1.7	1780 – 356
249.32 ± 0.03	35 ± 3.0	356 – 106	1460.6 ± 0.5	1.7 ± 0.5	1688 – 227
305.10 ± 0.18	1.4 ± 0.3	661 – 356	1466.26 ± 0.15	6.3 ± 0.5	2127 – 661
309.07 ± 0.09	3.5 ± 0.3	536 – 227	1530.50 ± 0.20	1.0 ± 0.5	2271 – 740
356.00 ± 0.20	2.7 ± 1.0	356 – 0	1537.85 ± 0.05	248 ± 5	1780 – 242
386.48 ± 0.09	3.3 ± 0.3	614 – 227	1552.18 ± 0.06	56.3 ± 1.4	1780 – 227
392.6 ± 0.4	0.6 ± 0.3	3475 – 3083	1620.22 ± 0.22	3.9 ± 0.4	3083 – 1463
396.54 ± 0.21	1.3 ± 0.3	933 – 536	1658.18 ± 0.06	34.0 ± 0.9	1780 – 121
419.12 ± 0.05	8.2 ± 0.3	661 – 242	1692.6 ± 0.5	2.0 ± 0.5	2433 – 740
429.93 ± 0.14	3.8 ± 0.8	536 – 106	1695.2 ± 1.9	0.33 ± 0.19	3475 – 1780
433.47 ± 0.05	33.5 ± 1.0	661 – 227	1751.0 ± 0.3	1.5 ± 0.3	3878 – 2127
433.9 ± 0.3	2.6 ± 0.8	676 – 242	1780.04 ± 0.06	172 ± 4	1780 – 0
465.28 ± 0.19	1.8 ± 0.3	3703 – 3238	1819.1 ± 0.3	1.9 ± 0.3	2433 – 614
470.34 ± 0.08	6.1 ± 0.4	712 – 242	1885.42 ± 0.15	5.8 ± 0.4	2127 – 242
476.10 ± 0.11	3.4 ± 0.3		1899.61 ± 0.16	4.9 ± 0.4	2127 – 227
492.63 ± 0.05	31.0 ± 0.8	614 – 121	1980.99 ± 0.15	4.4 ± 0.3	3083 – 1102
498.59 ± 0.12	3.9 ± 0.3	740 – 242	2006.00 ± 0.14	3.0 ± 0.5	2127 – 121
508.0 ± 0.3	1.6 ± 0.5	614 – 106	2127.52 ± 0.07	35.3 ± 1.2	2127 – 0
539.49 ± 0.04	790 ± 18	661 – 121	2149.51 ± 0.10	7.1 ± 0.3	2271 – 121
554.37 ± 0.05	130 ± 3	661 – 106	2160.9 ± 0.6	0.81 ± 0.24	3093 – 933
565.19 ± 0.08	5.3 ± 0.4	1102 – 536	2191.46 ± 0.25	2.9 ± 0.3	2433 – 242
569.20 ± 0.05	15.5 ± 0.5	676 – 106	2205.6 ± 0.6	1.0 ± 0.3	2433 – 227
577.1 ± 0.3	1.4 ± 0.4	933 – 356	2352.7 ± 0.4	2.3 ± 0.4	3093 – 740
585.86 ± 0.20	1.3 ± 0.2	1688 – 1102	2417.33 ± 0.23	4.9 ± 0.4	3093 – 676
614.38 ± 0.09	5.4 ± 0.4	614 – 0	2421.5 ± 0.8	1.3 ± 0.4	3083 – 661
619.08 ± 0.05	27.8 ± 0.8	740 – 121	2432.78 ± 0.21	3.9 ± 0.4	3093 – 661
621.3 ± 0.9	1.0 ± 0.7	3703 – 3083	2468.56 ± 0.11	12.0 ± 1.0	3083 – 614
626.49 ± 0.08	7.3 ± 0.5	1780 – 1153	2479.4 ± 0.7	1.0 ± 0.5	3093 – 614
658.1 ± 0.5	0.8 ± 0.3		2497.6 ± 1.5	0.4 ± 0.2	3238 – 740
661.23 ± 0.05	8.5 ± 0.3	661 – 0	2726.68 ± 0.11	22.4 ± 0.9	3083 – 356
677.69 ± 0.07	9.8 ± 0.5	1780 – 1102	2770.9 ± 0.4	1.5 ± 0.3	3703 – 933
690.72 ± 0.07	10.2 ± 0.4	933 – 242	2855.4 ± 0.3	8.3 ± 1.6	3083 – 227
705.47 ± 0.12	3.2 ± 0.3	933 – 227	2865.73 ± 0.21	4.8 ± 0.4	3093 – 227
731.33 ± 0.04	38.1 ± 1.0	838 – 106	2948.8 ± 0.5	1.0 ± 0.5	3625 – 676
739.0 ± 1.0	0.6 ± 0.2	1400 – 661	3010.3 ± 0.8	0.79 ± 0.25	3238 – 227
745.8 ± 0.4	1.6 ± 0.5	1102 – 356	3205.1 ± 0.6	0.89 ± 0.22	3881 – 676
925.49 ± 0.09	5.7 ± 0.4	1153 – 227	3217.1 ± 2.1	0.28 ± 0.22	3878 – 661
941.86 ± 0.05	34.3 ± 0.9	1780 – 838	3256.2 ± 1.2	0.53 ± 0.22	
947.6 ± 0.4	1.5 ± 0.5	1688 – 740	3269.0 ± 0.4	1.7 ± 0.3	3625 – 356
967.33 ± 0.11	5.5 ± 0.5	3238 – 2271	3344.3 ± 0.3	2.9 ± 0.4	3881 – 536
980.29 ± 0.11	4.8 ± 0.4	1102 – 121	3465.1 ± 0.9	0.9 ± 0.3	
1031.2 ± 0.3	1.6 ± 0.4	1153 – 121	3855.3 ± 0.4	3.1 ± 0.3	
1039.11 ± 0.08	10.7 ± 0.5	1780 – 740	4166.5 ± 1.0	0.8 ± 0.3	
1103.92 ± 0.07	8.8 ± 0.5	1780 – 676			

[a] The relative intensity can be converted to transitions per 100 β decays using the factor 0.0362, as calculated from the proposed decay scheme with a ground-state β branch of 29%.

TABLE II. Coincidences observed in the decay of ^{90}Kr.

Gating transition (keV)	Coincident transitions[a] (keV)
120.92	309, 433, 705, 925, 1118, 1552, 1899, 2205, 2855, 2865, 3010
121.81	106, 234, 492, 539, 619, 980, 1039, 1118, 1165, 1341, 1386, 1423, 1466, (1620), 1658, 1692, 1980, 2006, 2149; 2432, 2468, 2726
234.44	121, (180), (305), 677, 745, 1423, 1980, 2726, 3269
242.19	419, 433, 470, 498, 1118, 1537, 1885, 2191
249.32	(18), (305), 1423, 2726
433.47	120, 1118, (1303)
492.63	121, 1165, 1819, 2468, 2479
539.49	121, 1118, 1240, 1466, 2421, 2432
554.37	1118, (1466)
619.08	121, 1039, 1386, 1530, 1692, 2352
731.33	941
941.86	731
1118.69	121, 242, 419, 433, 539, 554, 661, (1303)
1423.77	121, 234, 249, 356
1537.85	242
2468.56	121, (392), 492

[a] Weakly indicated coincidences shown in parentheses.

IV. DISCUSSION

The β decay of even-even ^{90}Kr proceeds from the 0^+ state. Using the rules of Raman and Gove,[16] the logft values were used in association with the observed γ-ray transitions to deduce the level spin-parity assignments proposed in Fig. 4. The only unique spin assignments resulted either from the presence of allowed β transition logft values or from γ transition multipolarity information. In the former case, a spin-parity of 1^+ resulted, since a $0^+ \rightarrow 0^+$ β transition is excluded by the isobaric spin selection rule. This is illustrated, for example, in the assignment of 1^+ for the 1780-keV level.

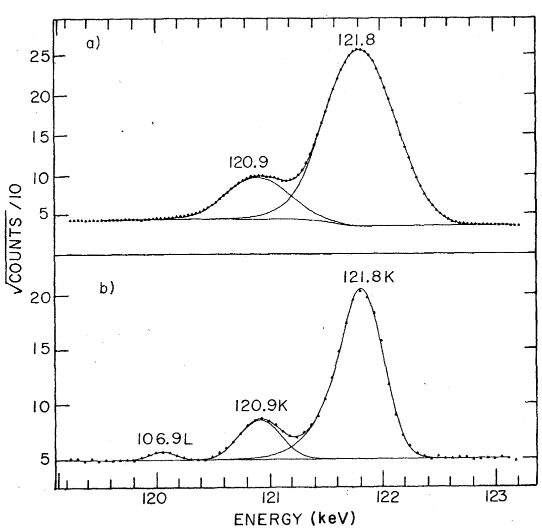

FIG. 2. High-resolution spectra showing the 121-keV doublet. (a) γ-ray spectrum; (b) conversion electron spectrum.

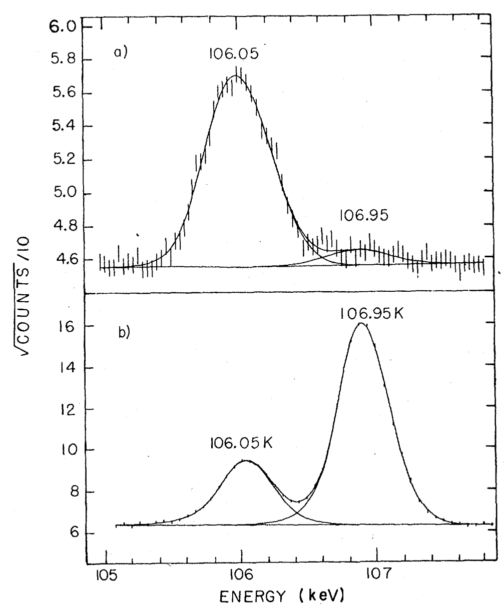

FIG. 3. High-resolution spectra showing the 106-keV doublet. (a) γ-ray spectrum; (b) conversion electron spectrum.

TABLE III. Internal conversion coefficient results.

E (keV)	Relative intensity I_γ	I_K	I_L	Conv. coeff.[a] α_K	α_L	Transition multipolarity
106.0	11.5 ± 0.7	2.54 ± 0.08		0.22 ± 0.06		$M1$ (21 ± 8)% $E2$
106.9	1.1 ± 0.3	9.72 ± 0.15	1.6[b] ± 0.3	8.84	1.4 ± 0.5	$M3$
120.9	90 ± 6	13.1[b] ± 0.9		0.15 ± 0.04		$M1$ (20 ± 12)% $E2$
121.8	910 ± 30	128[b] ± 7		0.14 ± 0.04		$M1$ (20 ± 12)% $E2$

[a] Obtained with 106.9-keV isomeric transition as pure $M3$.
[b] Intensities obtained using relation $(I_{120.9K}+I_{121.8K})/I_{106.9K}=14.6\pm0.5$ (Ref. 12).

The shell-model states available for low-lying levels of ^{90}Rb are $2d_{5/2}$, $3s_{1/2}$, and $1g_{7/2}$ particle states for the neutrons, and the $1f_{5/2}$, $2p_{3/2}$ hole, and $2p_{1/2}$ particle states for the protons. It is reasonable, therefore, to consider negative parity for these levels, which is supported by the known negative ground-state parities systematically exhibited for lower mass even-A Rb nuclei. Given the 0^- and 3^- character of the ^{90}Rb ground state and 106-keV level, respectively, the dominant $M1$ character of the 106.05-, 120.92-, and 121.82-keV transitions (see Table III) was used to deduce the unique spin-parity assignments of 1^- and 2^- for the 121- and 227-keV levels, respectively. Spin-parity ranges for many of the remaining levels were narrowed from the β branch $\log ft$ choices on the basis of observed γ-ray transitions to lower states, particularly the 2^- 227-keV level, or from higher 1^+ states, under the assumption that these transitions were restricted to $E1$, $M1$, or $E2$ multipolarity. These procedures have yielded a consistent, if not unique, set of spin-parity assignments for the proposed level scheme, given the lack of any reaction data for levels of ^{90}Rb.

From the systematics of odd-A Rb isotopes, a plausible shell-model configuration for the lowest states in ^{90}Rb is $\pi(1f_{5/2}^{-1})\nu(2d_{5/2}^{3})$. (The configurations expressed are relative to a $^{88}_{38}\mathrm{Sr}_{50}$ core.) According to the coupling rules of Brennan and Bernstein,[17] the proton-neutron coupling should result in 0^- or 5^- being preferred for the ground state. Obviously, the former is preferred. The states at 106, 121, and 227 keV appear to represent other couplings of the same configuration, since transitions between the four lowest states are predominantly $M1$ in character (except for the isomeric transition). The 4^- and 5^- states resulting from different couplings of this configuration are not expected to be noticeably populated in the β decay of 0^+ ^{90}Kr.

Very little can be said about the other levels in ^{90}Rb with the exception of the strongly β-fed 1^+ states. There appear to be two classes of 1^+ levels, separated roughly by 1 MeV and characterized by deexcitation patterns which differ. The 1780- and 2127-keV levels have $E1$ γ transitions to the 0^- ground state, while the levels at 3083, 3093, and 3238 keV have no ground-state γ transitions (the lowest level they populate is the 227-keV 2^- level).

For interpretation of the levels at 1780 and 2127 keV, not only must the allowed nature of the populating β transition be included, but also the $E1$ character of the depopulating γ transition to the ground state. A possible interpretation is obtained using a weak coupling scheme built from the levels of ^{89}Rb and ^{91}Sr, similar to the arguments employed in the interpretation of similar levels in ^{88}Rb.[18] Using the level schemes developed for ^{89}Rb and ^{91}Sr from the decays of ^{89}Kr and ^{91}Rb,[19,20] the $\frac{5}{2}^+$ 1693-keV level in ^{89}Rb could be coupled to the $\frac{5}{2}^+$ ground state of ^{91}Sr to provide a 1^+ level at about 1700 keV (neglecting the residual proton hole-neutron particle interaction). Similarly, a 1^+ level at about 2600 keV can be formed from coupling the $\frac{3}{2}^-$ ground state in ^{89}Rb with the $(\frac{1}{2}^-)$ 2657-keV level in ^{91}Sr. The combination mentioned are the lowest-energy possibilities for 1^+ levels under weak coupling.

Given the difficulty of obtaining more definitive information for ^{90}Rb by decay studies alone, it would be very useful to obtain more definitive information on the nature of the levels in ^{89}Rb and ^{91}Sr. The weak coupling interpretation presented above could perhaps be far less speculative with such information. If systematics can be used as a clue to the nature of the 1^+ levels, it is first evident that for odd-odd nuclei there is usually little systematic behavior to offer insight. However, as can be seen from Fig. 5, the two lowest-energy 1^+ levels which are also strongly β fed in the nuclei ^{88}Rb, ^{90}Rb, and ^{92}Rb,[21,22] exhibit similar characteristics. Each nucleus has a 1^+ level with $\log ft \simeq 4.5$, which is the dominant β branch of the associated even-even Kr parent. These 1^+ levels have a smooth decrease in excitation energy as neutron pairs are added to ^{88}Rb. In addition, each nucleus has a 1^+ level with $\log ft \simeq 5.8$; these 1^+ levels have a very slow decrease in excitation en-

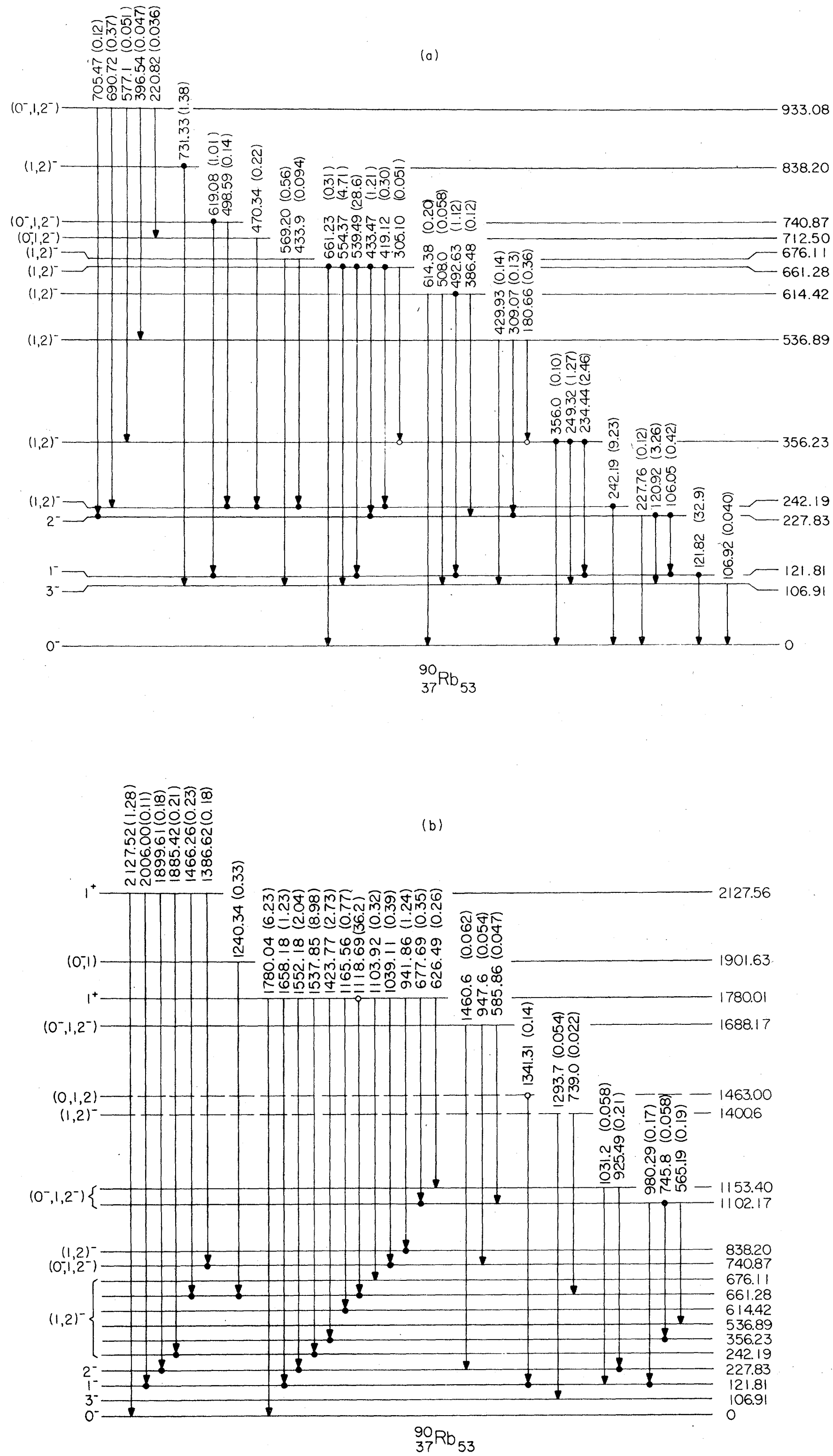

FIG. 4. Level scheme of ^{90}Rb populated in the decay of ^{90}Kr. Coincidences are indicated by filled circles at the transition start and termination points (probable coincidences, by open circles). (a) levels to 933 keV; (b) levels from 1102 to 2127 keV; (c) levels from 2271 to 3881 keV. Note that not all lower levels are shown in (b) and (c).

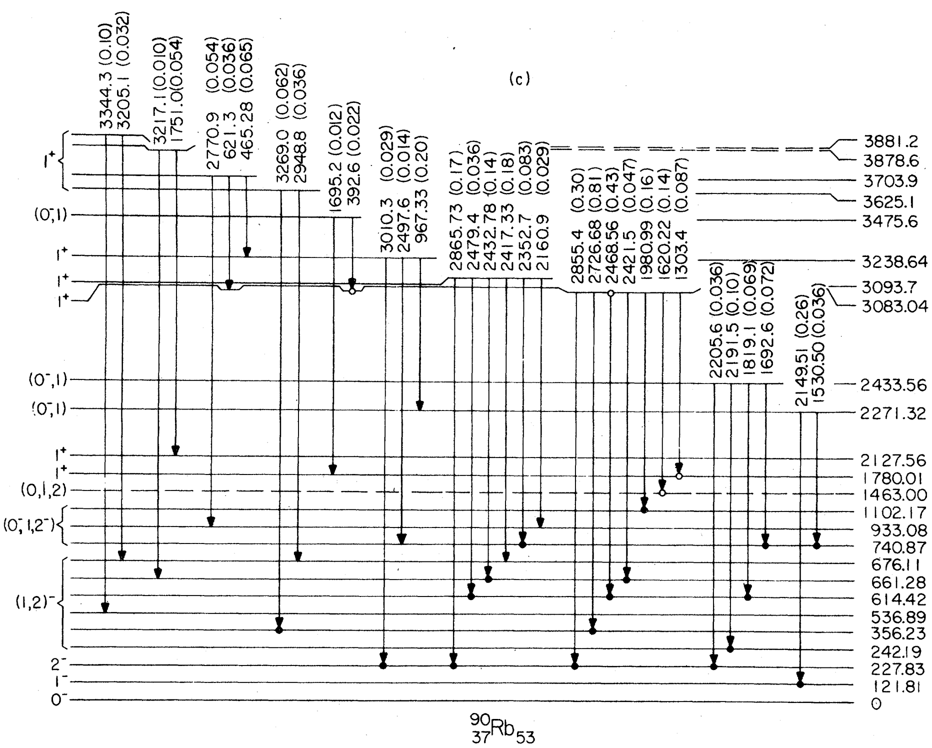

FIG. 4. *(Continued)*.

ergy. The apparent systematic trends of these 1^+ levels suggest configurations which differ only by pairs of zero-coupled neutrons.

In order to provide an interpretation of the systematic trends, based on the $\log ft$ values, of the 1^+ levels shown in Fig. 5, it is necessary to know the ground-state configurations for the three nuclei. For ^{88}Rb, the configuration $\pi(2p_{3/2}^{-1})\nu(2d_{5/2}^{1})$ is the dominant component, although the configuration $\pi(1f_{5/2}^{-1})\nu(2d_{5/2}^{1})$ can also be admixed.[18] Since the ground-state spins of ^{90}Rb and ^{92}Rb have recently been determined to be 0,[2,23] it is apparent that the proton hole is $1f_{5/2}$ and the odd neutron is $2d_{5/2}$. The $1f_{5/2}$ proton hole in the ground states of ^{90}Rb and ^{92}Rb occurs at a lower neutron number than one would expect from unperturbed weak coupling, since the ground-state spin values for the nuclei ^{89}Rb, ^{91}Rb, and ^{93}Rb are $\frac{3}{2}$, $\frac{3}{2}$, and $\frac{5}{2}$, respectively.[2,23]

The $E1$ γ-ray deexcitation patterns of the 1^+ levels shown in Fig. 5 must be taken into consideration in any proposed explanation of these systematic trends. The 1^+ levels with $\log ft \simeq 5.8$ deexcite primarily to the ground-state multiplet in all three cases. The 1^+, $\log ft = 4.4$ level at 2392 keV in ^{88}Rb has a deexcitation pattern similar to that of the 2231-keV level, whereas the corresponding levels with $\log ft \simeq 4.5$ in ^{90}Rb and ^{92}Rb have a deexcitation pattern dominated by a single γ ray. In ^{90}Rb, the 1118-keV γ transition carries 60% of the deexcitation intensity, and in ^{92}Rb the 1218-keV γ transition carries 67%. In order to understand the implications of these deexcitation patterns, one must first consider the possible allowed β and $E1$ γ mechanisms.

In the following decay mechanisms, only relatively simple configurations will be included. Since the goal is to provide an explanation for the trends, the configurations will be limited to those which can be easily extrapolated from ^{88}Rb to ^{90}Rb and ^{92}Rb by addition of zero-coupled pairs of $2d_{5/2}$ neutrons. Configurations are presented only for $A = 90$. There are two simple mechanisms involving the $1f_{5/2}$ protons for $0^+ \to 1^+$ β decay followed by $1^+ \to 0^-, 1^-, 2^-$ $E1$ γ decay:

$$\pi(1f_{5/2}^{-2})\nu(2d_{5/2}^{4}) \xrightarrow{\beta} \pi(1f_{5/2}^{-2}2d_{5/2}^{1})\nu(2d_{5/2}^{3}) \xrightarrow{\gamma} \pi(1f_{5/2}^{-1})\nu(2d_{5/2}^{3})_{0^- - 2^-}$$
$$\searrow_{\beta}\ \pi(1f_{5/2}^{-1})\nu(2d_{5/2}^{4}1f_{5/2}^{-1})\ \nearrow_{\gamma}\ .$$

There are two similar mechanisms involving the $2p_{3/2}$ protons:

$$\pi(2p_{3/2}{}^{-2})\nu(2d_{5/2}{}^{4}) \xrightarrow{\beta} \pi(2p_{3/2}{}^{-2}\,2d_{5/2}{}^{1})\nu(2d_{5/2}{}^{3}) \xrightarrow{\gamma} \pi(2p_{3/2}{}^{-1})\nu(2d_{5/2}{}^{3})_{1^-,2^-}$$

$$\searrow_{\beta}\ \pi(2p_{3/2}{}^{-1})\nu(2d_{5/2}{}^{4}\,2p_{3/2}{}^{-1})\ \nearrow_{\gamma}\ .$$

As indicated, the mechanisms involving the $2p_{3/2}$ protons would not populate the 0^- states.

Since the 1^+ states with $\log ft \simeq 5.8$ deexcite primarily to the ground states, their trend could be best understood with a $1f_{5/2}$ mechanism as the dominant decay path. The deexcitation to the 2^- ground state of ^{88}Rb could also follow this mechanism due to the possible admixtures for spin 2 of the configurations $\pi(2p_{3/2}{}^{-1})\nu(2d_{5/2}{}^{1})$ and $\pi(1f_{5/2}{}^{-1})\nu(2d_{5/2}{}^{1})$ in the ^{88}Rb ground state. Although other contributions to this decay cannot be excluded, this path is certainly the one most consistent with the apparent trend in the 1^+ levels with $\log ft \simeq 5.8$.

The trend of the 1^+ levels with $\log ft \simeq 4.5$ is more difficult to understand due to the differences in γ-ray deexcitation patterns for the three nuclei. If an explanation can be offered that involves changing only the zero-coupled pairs of neutrons, then the dominant decay path would involve the $2p_{3/2}$ protons. If the $1f_{5/2}$ proton mechanisms presented above were involved, then these 1^+ levels should deexcite primarily to the ground state (or other members of the ground-state configuration) which have an odd $1f_{5/2}$ proton. Since this is clearly not the case for ^{90}Rb, an explanation must be sought which would exclude the ground-state $E1$ γ transitions included in the $1f_{5/2}$ mechanisms. The $2p_{3/2}$ mechanisms could accomplish this in the following manner. If the dominant configuration of the level populated by the strong $E1$ γ ray from the 1^+ levels with $\log ft \simeq 4.5$ involved the $2p_{2/3}$ proton hole, i.e., $\pi(2p_{3/2}{}^{-1})\nu(2d_{5/2}{}^{3})$ in ^{90}Rb and $\pi(2p_{3/2}{}^{-1})\nu(2d_{5/2}{}^{5})$ in ^{92}Rb, then the strong $E1$ γ ray to such a state would be a natural consequence of the decay path involving the $2p_{3/2}$ proton. A small admixture in the 1^+ level of states involving the $1f_{5/2}$ proton would then allow weaker $E1$ γ transitions to the ground-state configuration.

The preceding explanation, which is quite speculative, could explain the trends observed in the two classes of 1^+ levels, with the low ($\simeq 4.5$) and high ($\simeq 5.8$) $\log ft$ 1^+ levels respectively dominated by configurations involving the $2p_{3/2}$ and $1f_{5/2}$ mechanisms. However, this implies quite different behaviors for the two mechanisms. The energy differences between the intermediate and final states in the $1f_{5/2}$ mechanism are essentially unaffected by the addition of neutron pairs. For the $2p_{3/2}$ mechanism, however, the energy difference between the intermediate and final states drops by a factor of 2 in going from ^{88}Rb to ^{90}Rb and then remains essentially unchanged in going to ^{92}Rb.

In conclusion, it is possible to offer an explanation for the apparent trends in 1^+ levels shown in Fig. 5 by means of simple configurations which differ only by zero-coupled pairs of $2d_{5/2}$ neutrons. The interpretation offered is, however, extremely speculative and not entirely satisfactory

TABLE IV. β branching and $\log ft$ values for ^{90}Kr decay.

Level energy (keV)	Percent branching	$\log ft$
0.0	29 ± 4	5.91 ± 0.06
106.91 ± 0.04	~0	...
121.81 ± 0.04	2.4 ± 1.4	6.9 ± 0.3[b]
227.83 ± 0.05	~0	...
242.19 ± 0.03	~0	...
356.23 ± 0.05	~0	...
536.89 ± 0.07	~0	...
614.42 ± 0.07	0.19 ± 0.06	7.81 ± 0.14[b]
661.28 ± 0.04	~0	...
676.11 ± 0.05	0.09 ± 0.05	8.10 ± 0.24[b]
712.50 ± 0.08	0.18 ± 0.03	7.78 ± 0.07[b]
740.87 ± 0.06	0.31 ± 0.06	7.53 ± 0.08[b]
838.20 ± 0.05	0.14 ± 0.05	7.82 ± 0.16[b]
933.08 ± 0.21	0.54 ± 0.05	7.19 ± 0.04[b]
1102.17 ± 0.11	~0	...
1153.40 ± 0.13	~0	...
1400.6 ± 0.3	0.08 ± 0.02	7.74 ± 0.11[b]
1463.00 ± 0.17	~0	...
1688.17 ± 0.19	0.16 ± 0.03	7.26 ± 0.08[b]
1780.01 ± 0.05	61 ± 4	4.61 ± 0.03
1901.63 ± 0.11	0.33 ± 0.03	6.79 ± 0.04
2127.56 ± 0.10	2.13 ± 0.14	5.81 ± 0.04
2271.32 ± 0.09	0.09 ± 0.03	7.11 ± 0.15
2433.56 ± 0.18	0.28 ± 0.03	6.43 ± 0.05
3083.04 ± 0.15	1.92 ± 0.14	4.89 ± 0.05
3093.7 ± 0.3	0.64 ± 0.05	5.36 ± 0.05
3238.64 ± 0.12	0.18 ± 0.03	5.71 ± 0.08
3475.6 ± 0.4	0.03 ± 0.01	6.11 ± 0.12
3625.1 ± 0.3	0.10 ± 0.02	5.30 ± 0.10
3703.9 ± 0.2	0.16 ± 0.03	4.93 ± 0.10
3878.6 ± 0.3	0.06 ± 0.01	4.91 ± 0.10
3881.2 ± 0.3	0.14 ± 0.02	4.53 ± 0.10

[a] Calculated using the proposed decay scheme and $Q_\beta = 4.39 \pm 0.04$ MeV.

[b] $\log f_1 t > 8.5$, so cannot exclude first-forbidden unique transition.

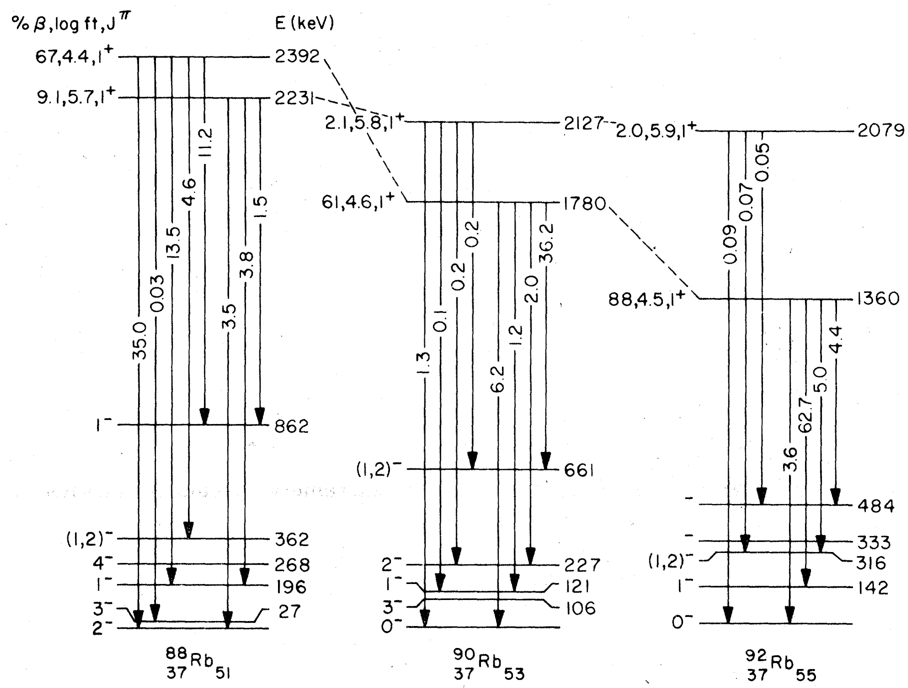

FIG. 5. Selected levels in ^{88}Rb, ^{90}Rb, and ^{92}Rb, showing systematic trends in the β-feeding and de-excitation patterns in the two lowest 1^+ states. Intensities for γ rays are per 100 decays. Not all levels below the 1^+ states are shown.

because the γ-ray deexcitation patterns are not naturally explained. Given our present knowledge of the levels involved, a more complete explanation cannot be offered. As stated previously, it would be very useful to have more definitive information on ^{89}Rb and ^{91}Sr, as well as ^{90}Rb, in order to provide less speculative explanations for the structures of the strongly β-fed 1^+ levels.

We wish to express our appreciation to J. R. McConnell, J. J. Eitter, and R. J. Olson for assistance in acquisition and analysis of the data, and to J. P. Vary and B. J. Dalton for discussions regarding interpretation of the levels. One of the authors (C.L.D.) would like to acknowledge the support of the Alfred P. Sloan Foundation through its grant to Grinnell College.

*Present address: Los Alamos Scientific Laboratory, P. O. Box 1663, Los Alamos, N. M. 87545.

[1]J. F. Mason and M. W. Johns, Can. J. Phys. 48, 2056 (1970).
[2]C. Ekström, S. Ingelman, G. Wannberg, and M. Skarestad, Hyperfine Interactions 4, 165 (1978).
[3]D. C. Kocher, Nuclear Data Sheets 16, 55 (1975).
[4]F. K. Wohn, M. D. Glascock, W. L. Talbert, Jr., S. T. Hsue, and R. J. Hanson, Phys. Rev. C 13, 2492 (1976).
[5]G. H. Carlson, W. C. Schick, Jr., W. L. Talbert, Jr., and F. K. Wohn, Nucl. Phys. A125, 267 (1969).
[6]F. K. Wohn and W. L. Talbert, Jr., Phys. Rev. C 18, 2328 (1978).
[7]F. K. Wohn, in Proceedings of the Isotope Separator On-Line Workshop, edited by R. E. Chrien, BNL Report No. 50847, 1978 (unpublished), p. 23.
[8]W. L. Talbert, Jr., F. K. Wohn, John C. Hill, A. R. Landin, M. A. Cullison, and R. L. Gill, Nucl. Instrum. Methods (to be published).
[9]J. R. McConnell and W. L. Talbert, Jr., Nucl. Instrum. Methods 128, 227 (1975).
[10]E. A. Henry, W. L. Talbert, Jr., and J. R. McConnell, Phys. Rev. C 7, 222 (1973).
[11]J. K. Halbig, F. K. Wohn, and W. L. Talbert, Jr., Rev. Sci. Instrum. 45, 789 (1974).
[12]J. K. Halbig, Ph.D. thesis, Iowa State University, 1973 (unpublished).
[13]H. Huang, B. P. Pathak, R. Iafigliola, L. Lessard, and J. K. P. Lee, Z. Phys. A282, 285 (1977).
[14]R. S. Hager and E. C. Seltzer, Nucl. Data Sect. A 4, 35 (1968).
[15]I. Amarel, R. Bernas, R. Foucher, J. Jastrzebski, A. Johnson, J. Teillac, and H. Gauvin, Phys. Lett. 243, 402 (1967).
[16]S. Raman and N. B. Gove, Phys. Rev. C 7, 1995 (1973).
[17]M. H. Brennan and A. M. Bernstein, Phys. Rev. 120, 927 (1960).
[18]R. L. Bunting, W. L. Talbert, Jr., J. R. McConnell, and R. A. Meyer, Phys. Rev. C 13, 1577 (1976).
[19]E. A. Henry, W. L. Talbert, Jr., and J. R. McConnell, Phys. Rev. C 7, 222 (1973).
[20]M. D. Glascock, W. L. Talbert, Jr., and C. L. Duke, Phys. Rev. C 13, 1630 (1976).
[21]R. J. Olson, W. L. Talbert, Jr., and J. R. McConnell, Phys. Rev. C 5, 2095 (1972).
[22]J. R. Clifford, W. L. Talbert, Jr., F. K. Wohn, J. P. Adams, and J. R. McConnell, Phys. Rev. C 7, 2535 (1973).
[23]C. Ekström, private communication.